Carcinogenesis vol.35 no.9 pp.2007–2013, 2014
doi:10.1093/carcin/bgu087
Advance Access publication April 11, 2014

ATM-mediated Mad1 Serine 214 phosphorylation regulates Mad1 dimerization and the spindle assembly checkpoint

Chunying Yang[1,2], Jianwei Hao[1,3], Dejuan Kong[1,4], Xiaoli Cui[2], Wei Zhang[5], Haibo Wang[1], Xiaojing Guo[1], Shumei Ma[4], Xiaodong Liu[4], Peiyu Pu[3] and Bo Xu[1,2,6,*]

[1]Department of Radiation Oncology, Houston Methodist Hospital Research Institute, Houston, TX 77030, USA, [2]Department of Oncology, Drug Discovery Division, Southern Research Institute, Birmingham, AL 35205, USA, [3]Department of Neurosurgery, Tianjin Medical University General Hospital, Tianjin 300052, China, [4]Laboratory of Radiobiology, Jilin University School of Public Health, Changchun 130001, China, [5]Department of Medicinal Chemistry, Southern Research Institute, Birmingham, AL 35205, USA and [6]Cancer Cell Biology Program, Comprehensive Cancer Center, University of Alabama at Birmingham, Birmingham, AL 35205, USA

*To whom correspondence should be addressed. Tel: +1 205 581 2845;
Fax: +1 204 581 2097;
Email: xu@sri.org

The spindle assembly checkpoint (SAC), which blocks anaphase onset until all chromosomes have bi-oriented, is one of the key self-monitoring systems of the eukaryotic cell cycle for genome stability. The mitotic arrest-deficient protein 1 (Mad1), a critical component of the SAC, is hyperphosphorylated in mitosis. However, the kinases responsible for Mad1 phosphorylation and its functional significance are not fully understood. Here we report that Mad1 is phosphorylated on Serine 214 by the Ataxia-Telangiectasia Mutated (ATM) kinase, a critical DNA damage response protein also activated in mitosis and required for the SAC. We demonstrate that Mad1 Serine 214 phosphorylation promotes the formation of homodimerization of Mad1 and its heterodimerization with Mad2. Further we show that Mad1 Serine 214 phosphorylation contribute to activation of the SAC and the maintenance of chromosomal stability. Together, these findings reveal an important role of ATM-mediated Mad1 Serine 214 phosphorylation in mitosis.

Introduction

The precise partition of sister chromosomes to daughter cells is regulated by the spindle assembly checkpoint (SAC) in mitosis and essential for the maintenance of genome stability (1). Defects in SAC result in aneuploidy, which is well documented in a majority of tumor cells (2). In prometaphase of the cell cycle, unattached kinetochores recruit evolutionally conserved proteins such as Aurora-B, Bub1, Bub3, BubR1/Mad3, Mad1, Mad2 and MPS1 for activation of the SAC to prevent cells entering anaphase (3). In mammalian cells, Mad1 tightly associates with Mad2, forming a core complex required for activation of SAC. During mitosis, Mad1 localizes to kinetochore to facilitate the Mad2's inhibitory role of the anaphase promoting complex and it in turn triggers mitotic arrest (4). Elevated expression of Mad1 has been reported in cancer tissues (5). Upregulation of Mad1 can lead to mislocalization of Mad2, causing SAC defects and chromosomal instability (5). Meanwhile, reduced Mad1 function is also linked to an increased rate of cancer in mice (6). Mad1 is a phospho-protein during mitosis (7). Mad1 hyperphosphorylation is associated with overexpression of polo-like kinase one (8). A potential phosphorylation site (threonine 680) by polo-like kinase one is located on the C-terminal domain that has been reported to be important for its kinetochore localization (8). Structure of the Mad1 C-terminal domain reveals a homodimer with multiple *quasi*-independent kinetochore binding interfaces on the C-terminus (9). In contrast, the N-terminus of Mad1 serves as a species-specific determinant influencing the stringency of cellular responses to microtubule depolymerization and spindle damage (10).

In eukaryotic cells, another mechanism that guards against genome instability is the DNA damage response (DDR) (11). Orchestrated by a comprehensive network, an optimal DDR is required for detection of DNA damage caused by endogenous and exogenous insults and for coordination of DNA repair processes. There is growing evidence that many proteins involved in the DDR play roles in the SAC. For example, Ataxia-Telangiectasia Mutated (ATM) (12), Brca1 (13–15), Brca2 (16), Chk1 (17) and Chk2 (13,15) are components of SAC regulation. Among them, the ATM kinase is activated in mitosis in the absence of DNA damage by Aurora-B mediated Serine 1403 phosphorylation (12). ATM participates in SAC activation partially by regulation of Bub1 activity (12,18). However, a more comprehensive mechanism on how ATM regulates the SAC remains to be fully explored. In this report, we demonstrate that mitotically activated ATM phosphorylates Mad1 on Serine 214 to facilitate the SAC.

Abbreviations: ATM, Ataxia-Telangiectasia Mutated; DDR, DNA damage response; GST, glutathione-S-transferase; HA, hemagglutinin epitope; PBS, phosphate-buffered saline; SAC, spindle assembly checkpoint; shRNA, small hairpin RNA; WT, wild-type.

Materials and methods

Cell lines and culture

HeLa and HCT116 cells (American Type Culture Collection, Manassas, VA) were maintained in Dulbecco's modified Eagle's medium containing 10% fetal bovine serum and supplemented with 4 mM of L-glutamine and 50 μg/ml of penicillin/streptomycin (all from HyClone Laboratories) in 5% CO_2 at 37°C. The isogenic cell lines expressing control or ATM small hairpin RNA (shRNA) were maintained in Dulbecco's modified Eagle's medium supplemented with 1 μg/ml puromycin. The simian virus 40-transformed human fibroblast cell lines GM0637 and GM9607 cells (The NIGMS Human Mutant Cell Repository, Camden, NJ) were maintained in Roswell Park Memorial Institute 1640 medium supplemented with 10% fetal bovine serum and 50 μg/ml of penicillin/streptomycin.

Flow cytometry

For flow cytometry analyses, cells were harvested and fixed in 70% ethanol. After permeabilizing with 0.1% triton X-100 on ice for 5 min and blocking in phosphate-buffered saline (PBS) with 1% bovine serum albumin for 30 min, the fixed cells were incubated with the anti-phospho-histone-H3-Ser10 for 3 h at room temperature and the fluorescein isothiocyanate-conjugated secondary antibody for 30 min in the dark. Then cells were stained with 25 μg/ml propidium iodide (Life Technology, Grand Island, NY) and the percentage of mitotic cells was quantified using a FACS Calibur flow cytometer (Becton Dickinson) with CellQuest software.

Plasmids, antibodies and reagents

To make hemagglutinin epitope (HA)-tagged Mad1, the full-length coding sequences of Mad1 were obtained by reverse transcription–PCR and subcloned into the pCDNA3.1 vector at the BamHI-XbaI sites. The primers are 5′-actggatccacgatgTACCCATACGATGTTCCAGATTACGCTatggaagacctgggggaaaa cacca-3′ and 5′-agctctagactacgccacggtctggcggctgaagag-3′. The Flag-tagged Mad1 was subcloned into the pcDNA3.1 vector with the primers: 5′-actggatccacgatg ATGGACTACAAGGACGATGACGACAAGatggaagacctgggggaaaacacca-3′ and 5′-agctctagactacgccacggtctggcggctgaagag-3′. The Mad1-S214A mutant was generated using the QuikChange II XL site-directed mutagenesis kit (Stratagene) according to the manufacturer's protocol. The primers used are 5′-gaactccaggccgcacaagaagc aagagcagaccacgagcagc-3′and 5′-gctgctcgtg-gtctgctcttgcttcttgtgcggcctggagttc-3′. The primers for S214E mutation are 5′-gaa ctccaggccgagcaagaagcaagagcagac-3′ and 5′-gctgctcgtggtctgctcttgcttctt-gctcggcctggagttc-3′. The rabbit phospho-Mad1-S214 antibodies were raised against peptide KIQELQASpQEARA-NH2 in Abgent (San Diego, CA). Anti-Mad1, anti-Bub1, anti-INCENP and HA antibodies were bought from Abcam (Cambridge, MA). The anti-Flag antibody was obtained from OriGENE (Rockville, MD), and anti-histone-H3-Ser10p was from Millipore (Billerica, MA). The anti-Mad2 antibody was from Santa Cruz Biotechnology.

Live cell time-lapse imaging

The vector, wild-type (WT) and S214A Mad1 constructs were cotransfected with GFP-tagged H2B plasmid (AddGene, Cambridge, MA) using FuGENE

HD transfection reagent. Forty-eight hours later, the chromosome dynamics and mitotic timing were monitored every 15 min for 24 h in the IncuCyte system. All images were analyzed with the IncuCyte software and Image J.

Cytogenetic analysis

HCT116 cells were transfected with vector only, HA-Mad1-WT and HA-Mad1-S214A. 48 h later, cells were incubated with 100 ng/ml Colcemid (IrvineScientific, Santa Ana, CA) for 3 h and resuspended in warm hypotonic buffer (75 mM KCl) for 10 min at 37°C. Then cells were fixed by addition of cold methanol/acetic acid (3:1 v/v) and washed by fresh fixative agent twice followed by resuspension in the 300 µl fixative agent. The cells were then dropped onto the microscope slide from a height of 2 ft. The slides were air-dried and stained with 3% Giemsa in PBS for 10 min. Chromosome numbers were evaluated using a microscope under the ×100 objective.

Immunofluorescence

Cells were fixed in 4% paraformaldehyde for 15 min at room temperature and blocked with 1% bovine serum albumin in PBS for 30 min. Antibodies against Mad1 S214p and INCENP were incubated at 4°C overnight. After rinsing three times in PBS for 5 min each, cells were then incubated with fluorescence-conjugated secondary antibodies for 1 h. After washing three times with PBS, 4′,6-diamidino-2-phenylindole (0.5 µg/ml) was added to stain the cell nuclei. Then the coverslips were mounted onto glass slides and subjected to microscopy with an Olympus microscope DP71.

Immunoprecipitation and western blot

For immunoprecipitation with the anti-Flag antibody, whole cell lysates were incubated with anti-FLAG-M2 Agarose beads (Sigma, St Louis, MO) overnight at 4°C, washed three times with 500 µl Tris-buffered saline and then eluted in 80 µl Laemmli buffer. For HA immunoprecipitation, HA Tag IP/Co-IP kits were purchased from Pierce and performed according to the manufacturer's protocol. The eluted proteins were analyzed on an sodium dodecyl sulfate–polyacrylamide gel electrophoresis gel followed by probing with indicated antibodies. For general western blot analyses, protein samples were separated by sodium dodecyl sulfate–acrylamide and transferred to the nitrocellulose membrane. After incubating with primary and secondary antibodies, the signals were filmed and detected using the Pierce chemiluminescence detection system.

In vitro *kinase assays*

The ATM *in vitro* kinase assay was performed according to the standard methods described previously (18). Briefly, purified glutathione-S-transferase (GST)–ATM-N (N-terminal, a.a. 248–522) and GST–ATM-C (C-terminal, a.a. 2709–2964) proteins were incubated with non-phosphorylated Mad1 peptides in the kinase buffer (25 mM Tris–Hcl (pH 7.5), 5 mM β-glycerophosphate, 2 mM dithiothreitol, 0.1 mM Na3VO4, 10 mM MgCl2, 10 mM Mn2Cl2) with 5 mM adenosine triphosphate for 1 h at 30°C. After boiling for 5 min, the samples were fractionated on sodium dodecyl sulfate–polyacrylamide gel electrophoresis followed by Coomassie Blue staining and western blot analysis using the anti-Mad1 Serine 214p antibody.

Molecular modeling

Molecular modeling was performed using Schrödinger® suite 2012. Based on the crystal structure of pyruvate kinase (PDB ID: 1E0T), which shares 30% identical residues and 47% homologous residues with the Mad1 fragment (amino acids: 195–253), a homolog model was first generated using *PRIME*, the protein structure prediction module of Schrödinger®. This structural model of Mad1 fragment was then further optimized using the protein preparation protocol for final analysis.

Statistical analysis

All the data for the statistical analysis are obtained from at least three independent experiments. The unpaired Student's *t*-test was used for the significance analysis. Values of $P \leq 0.05$ were considered to be significant.

Results

Mad1 Serine 214 is phosphorylated by ATM in mitosis

We have recently demonstrated that the ATM kinase is activated in mitosis in an Aurora-B dependent manner (12). A large-scale phosphoproteomics study has indicated that Mad1 is one of the four mitotic factors that are downstream targets of ATM in the DDR (19). To test potential Mad1 phosphorylation by ATM in mitosis, we generated a phospho-specific antibody-recognizing Mad1 phosphorylation on Serine 214 (Supplementary Figures S1, available at *Carcinogenesis* Online). Using this antibody, we assessed Mad1 Serine 214 phosphorylation in simian virus 40-transformed fibroblast cell lines with proficient (GM0637) or deficient (GM9607) ATM after they were treated with a mitotic spindle-damaging agent nocodazole (200 nM, 16 h). As shown in Figure 1A, we detected a phosphorylation signal in GM0637 cells exposed to nocodazole. In contrast, GM9607 cells did not show nocodazole-induced Mad1 Serine 214 phosphorylation, suggesting a role of ATM in the process. It is noted the specificity of the phospho-antibody was demonstrated using immunoprecipitation experiments in HeLa cells transfected with vector, HA-tagged WT or the Serine 214 to alanine mutant form of Mad1 (S214A). Mutation of Serine 214 to alanine completely abrogated the phosphorylation signal (Supplementary Figure S1C, available at *Carcinogenesis* Online), and Mad1 knock-down by small interfering RNA diminished the signal of the Mad1 phospho-specific antibody in fluorescence microscopy (Supplementary Figure S1D, available at *Carcinogenesis* Online).

To further test whether Mad1 Serine 214 phosphorylation is dependent on ATM, we used a pair of the isogenic HeLa cell lines in which ATM has been stably transfected with control or ATM shRNA (12). We found that control shRNA cells displayed strong phosphorylation signals in response to nocodazole treatment. However, ATM shRNA infected cells showed defective Mad1 Serine 214 phosphorylation (Figure 1B and supplemental supplementary Figure 1B, available at *Carcinogenesis* Online—whole-gel blot). These data demonstrate that mitotic Mad1 Serine 214 phosphorylation is dependent on ATM.

To further test whether ATM directly phosphorylates Mad1, we utilized an *in vitro* kinase assay system in which GST–ATM C-terminus (GST–ATM-C) was incubated with Mad1 peptides containing the Serine 214 sequence. We found that, when non-phospho-Mad1 peptides were incubated with GST–ATM-C, a strong phosphorylation signal was observed (Figure 1C and Supplemental Supplementary Figure S2, available at *Carcinogenesis* Online—whole-gel blot), indicating that *in vitro* phosphorylation occurred. Together, our data demonstrate that ATM phosphorylates Mad1 on Serine 214 in mitosis.

Mad1 Serine 214 phosphorylation contributes to activation of the SAC

To study the functional significance of Mad1 Serine 214 phosphorylation, we tested whether or not overexpression of the WT or S214A mutant Mad1 would affect activation of the SAC. We transiently transfected vector-only, HA-tagged WT, or S214A Mad1 plasmids into HeLa cells. In response to nocodazole treatment, vector-only cells displayed time-dependent mitotic arrest quantified by flow cytometry of histone-H3-Serine 10 phosphorylation. However, in cells transfected with WT Mad1, activation of the SAC was significantly impaired. This observation is consistent with previous reports that overexpression of Mad1 might sequester Mad2 functions, therefore affecting activation of the SAC (5). Interestingly, we observed that expression of the Serine 214 to alanine mutant Mad1 resulted in a more significant reduction of mitotic arrest (Figure 2A).

We also conducted time-lapse microscopy for cells transfected with vector, WT or S214A (Figure 2B). We found that the mitotic timing was significantly shortened in cells expressing WT or S214A Mad1. However, S214A expression showed a more significant decrease in mitotic timing (Figure 2C). These results indicate that that Serine 214 phosphorylation influences the activation of SAC activation of the SAC.

We then conducted a cytogenetic analysis assessing chromosomal stability in cells expressing the WT or S214A mutant Mad1. We found that overexpressing either WT or S214A in HCT116 cells significantly increased the number of aneuploidy cells (Figure 2D and E). Although overexpressing WT Mad1 increased aneuploidy, cells with the S214A mutation possessed a significant higher number of aneuploidy ($P = 0.024$) compared with that of the WT Mad1. These observations indicate that the level of Mad1 must be tightly regulated to prevent aneuploidy and that Mad1 Serine 214 phosphorylation contributes to the maintenance chromosomal stability.

We also conducted a complementation experiment by introducing HA-tagged WT, S214A or S214E (the seine to glutamic acid

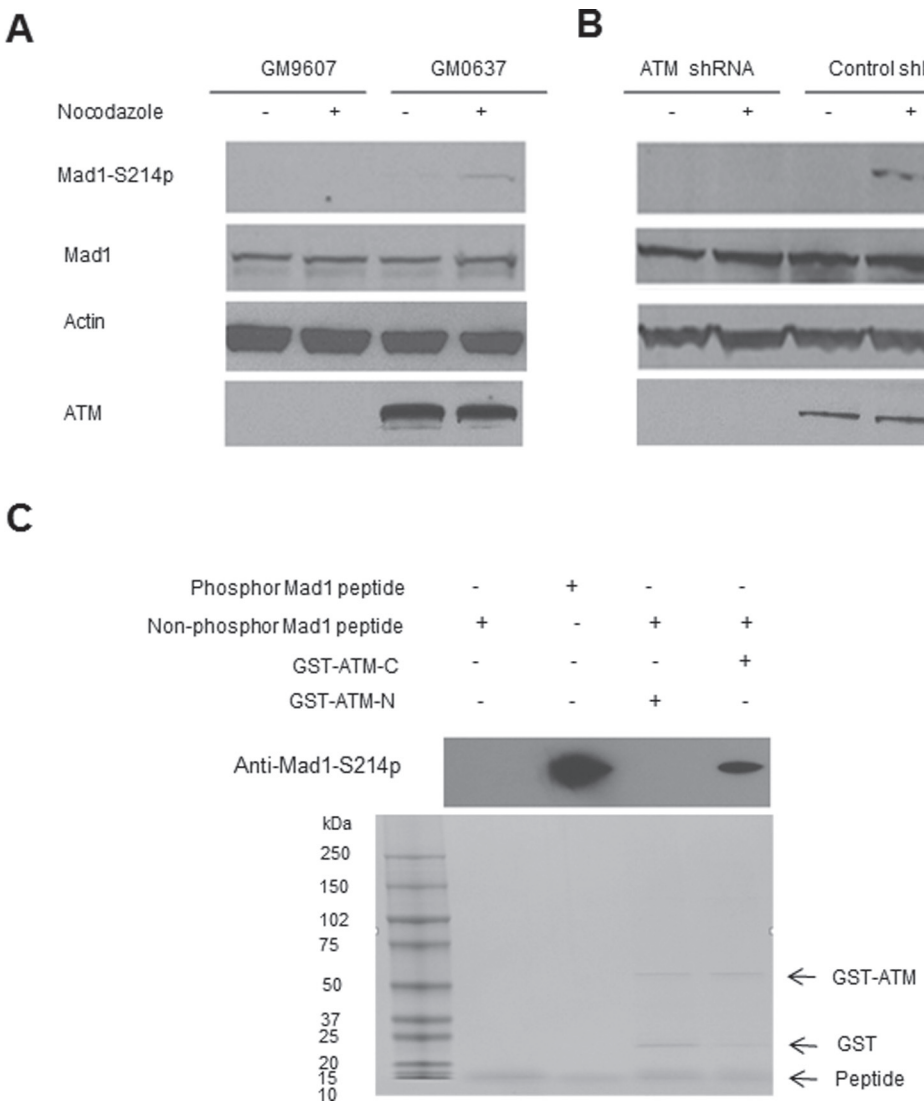

Fig. 1. ATM phosphorylates Mad1 on Serine 214 in mitosis. Immunoblotting with indicated antibodies in simian virus 40-transformed fibroblast cell lines GM0637 and GM9607 (**A**) and isogenic HeLa cell lines stably infected with control or ATM shRNA (**B**) in the absence or presence of nocodazole. (**C**) Phospho- or non-phospho-Mad1-Serine 214 peptides were incubated with the recombinant GST–ATM-C, which contains the kinase domain, in the presence of adenosine triphosphate. The GST–ATM-N terminal protein was used as a negative control. The upper blot was immunoblotted with the anti-phospho Serine 214 Mad1 antibody. Shown in the bottom blot was the Coomassie Blue staining of the purified proteins and peptides.

mutation) into control or ATM shRNA cells (Figure 2F). Interestingly, we found that cells expressing S214E partially displayed a less severe defect in the SAC with the ATM knock-down background, indicating a partial complementation effect of S214E.

Mad1 Serine 214 phosphorylation promotes Mad1 homodimerization and heterodimerization with Mad2

Since Mad1 functions in cells as homodimers and it also forms heterodimers with Mad2 (tetramer), we further hypothesized that ATM-mediated Mad1 Serine 214 phosphorylation might promote dimerization of Mad1. To test this possibility, we immunoprecipitated HA-tagged WT, S214A and S214E of Mad1 and immunoblotted the precipitates with anti-HA or Mad2 antibodies. As shown in Figure 3A, unlike with WT and S214E, Mad2 binding with Mad1-S214A was significantly reduced. These results suggest that Serine 214 phosphorylation is required for Mad1 and Mad2 binding. Further supporting this conclusion is that depletion of ATM reduces Mad1 and Mad2 binding (Figure 3B). It is noted that the endogenous Mad2 expression was not affected by Mad1 expression (Supplementary Figure S3, available at *Carcinogenesis* Online).

To test whether Serine 214 phosphorylation might affect Mad1 homodimer formation, we generated Flag-tagged Mad1 (WT or S214A) expression constructs. We cotransfected the Flag-tagged constructs with HA-tagged WT Mad1 into HeLa cells and conducted coimmunoprecipitation experiments. Interestingly, we found that Flag-tagged S214A binding with HA-tagged WT Mad1 was significantly reduced (Figure 3C). We also conducted a reciprocal experiment by introducing HA-tagged Mad1 (WT or S214A) with Flag-tagged WT Mad1 into HeLa cells. Similarly, we observed that HA-tagged S214A association with Flag-tagged WT Mad1 was significantly reduced. Together, these experiments indicate that Serine 214 phosphorylation of Mad1 promotes homodimerization of Mad1 and heterodimerization of Mad1 with Mad2.

ATM-mediated Mad1 and Bub1 phosphorylations are independent events during activation of the SAC

We previously reported that Bub1 Serine 314 is phosphorylated by ATM in mitosis and in response to DNA damage and that ATM-mediated Serine 314 phosphorylation is required for mitotic activation of Bub1 (18). To test whether ATM-mediated Mad1 phosphorylation

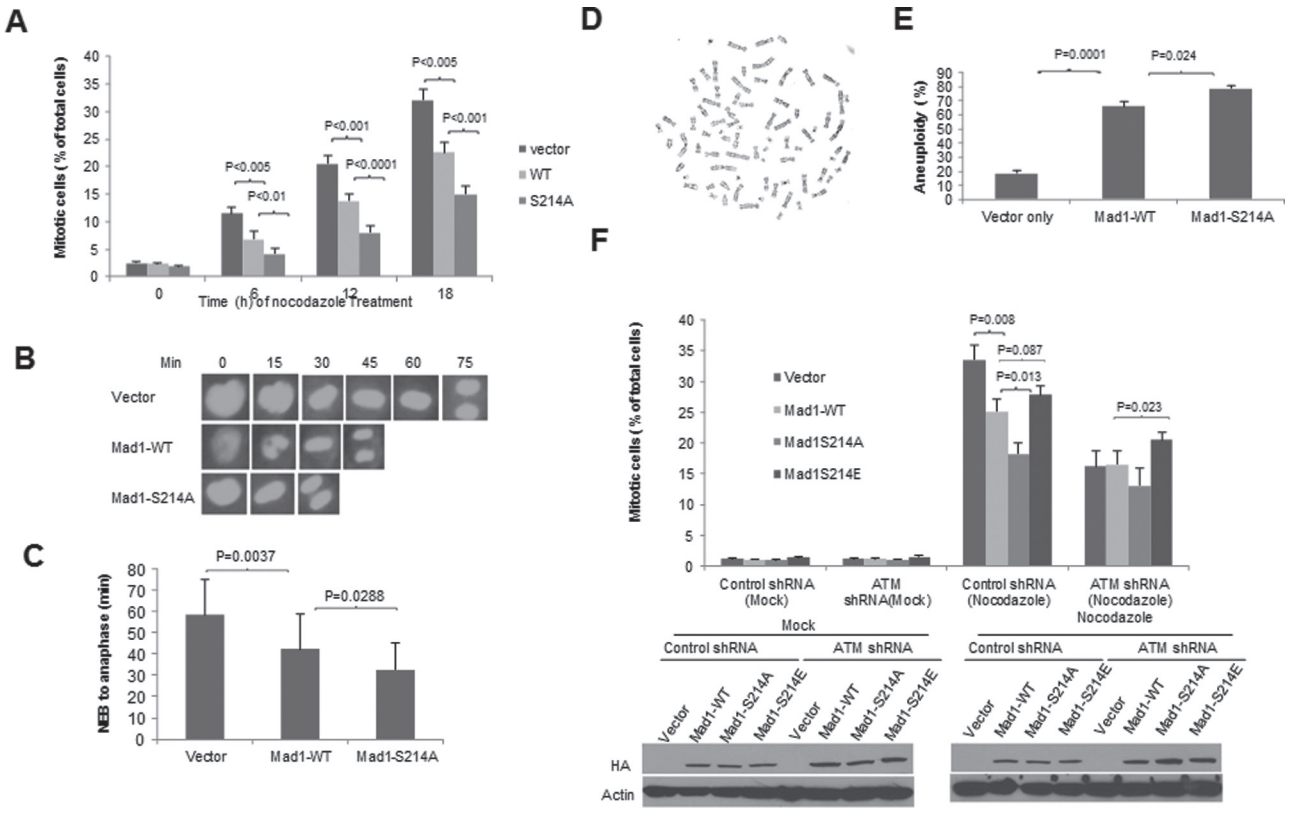

Fig. 2. Mad1 Serine 214 phosphorylation is involved in activation of the spindle checkpoint. (**A**) HeLa cells transfected with vector, the WT or S214A mutant form of Mad1 were exposed to nocodazole for the indicated times before they were harvested and stained with a flow cytometry-based histone-H3p antibody to determine the mitotic index. (**B**) Vector, Mad1-WT or Mad1-S214A plasmids were cotransfected with the H2B-GFP plasmids into HeLa cells. The time from nuclear envelop break down to anaphase onset was measured by time-lapse microscopy. (**C**) Mean mitotic timing are shown representing the average of ~20 mitotic cells in each group. Statistic analyses were done by *t*-test and *P* values are presented. (**D**) Representative image of aneuploidy. (**E**). HCT116 cells expressing HA-Mad1-S214A have higher levels of aneuploidy than cells expressing HA-Mad1-WT that have higher levels than control cells. (**F**) Vector, WT, S214A or S214E mutants of Mad1 were transfected into HeLa cells stably expressing control or ATM shRNA. The cells were treated with nocodazole for 16h followed by flow cytometric anti-phospho-H3 staining. In A and F, mean mitotic percentages of at least triplicate samples are shown, and error bars represent the variations around the averages. Statistic analyses were done by *t*-test and *P* values are presented.

is required for Bub1 Serine 314 phosphorylation or *vice versa*, we transfected Flag-tagged Bub1 (WT or S314A) into HeLa cells and measured Mad1 Serine 214 phosphorylation. We have shown previously that Bub1 S314A has a dominant negative effect; however, we found that Mad1 Serine 214 phosphorylation induced by nocodazole was not affected by Bub1 S314A expression (Figure 4A). Similarly, when HA-tagged Mad1 proteins were expressed in HeLa cells, Bub1 Serine 314 phosphorylation was not affected (Figure 4B). Therefore, these results indicate that Mad1 Serine 214 phosphorylation and Bub1 Serine 314 phosphorylation, both regulated by mitotic-activated ATM, function independently in regulating the activation process of the SAC. Interestingly, coexpression of Mad1 and Bub1 mutants in HeLa cells resulted in a more significant defect in the SAC (Figure 4C). It is noted that, in the absence of nocodazole, Bub1 S314A expression caused slight increase in Mad1 Serine 214 phosphorylation in the absence of nocodazole treatment.

A computational model of Mad1 Serine214 phosphorylation

Recent reports have revealed the structure of the Mad1 C-terminal domain as a homodimer with multiple *quasi*-independent kinetochore binding interfaces (9). However, the structure of the N-terminus of Mad1 remains unclear. Based on the crystal structure of pyruvate kinase (PDB ID: 1E0T), which shares 47% homologous residues with a human Mad1 fragment containing Serine 214, we generated a structural model of the Mad1 fragment (amino acids: 195–253). We found that Serine 214, along with two other conserved residues lysine 246 (K246) and arginine 251 (R251), could play a critical role on Mad1's function (Figure 5). In this structural model, Serine 214 locates at the tip of a loop region that is stabilized by electrostatic interactions between Serine 214 and K246/R251 and potential water-mediated hydrogen bonds. Specifically, Serine 214 is fully exposed, which facilitates kinase approaching and Serine 214 phosphorylation, the phosphorylated form of Serine 214 could further stabilize this conformation by strengthening the interactions with K246/R251. S214A mutation disables the phosphorylation at position 214 and at the same time loses these spatial interactions (electrostatic and hydrogen bonds), causing the loop to become highly flexible and affect the overall protein structure stability.

Discussion

Mad1 and Mad2 are two critical mitotic SAC proteins. In the event of insufficient proper microtubule attachments, Mad1 and Mad2, in a format of the core tetramer, are recruited to kinetochores and convert Mad2 from an open form to a closed form, and the latter one blocks anaphase entry by inhibiting the activation of anaphase promoting complex (20). In addition to the Mad2 complex dynamics, activities of widely conserved kinases, such as Aurora kinases, MPS1 and BubR1 are critical for the fidelity of cell division (21). Our results presented here highlight a critical pathway that is governed by the mitotically activated ATM kinase and phosphorylation of Mad1 on Serine 214. Serine 214 phosphorylation in the N-terminal region of Mad1 promotes Mad1 homodimerization and heterodimerization with Mad2 and it contributes to the activation of the SAC.

Our data showed that, in cells when both endogenous Mad1 and Mad2 are present, overexpression of the WT Mad1 compromises

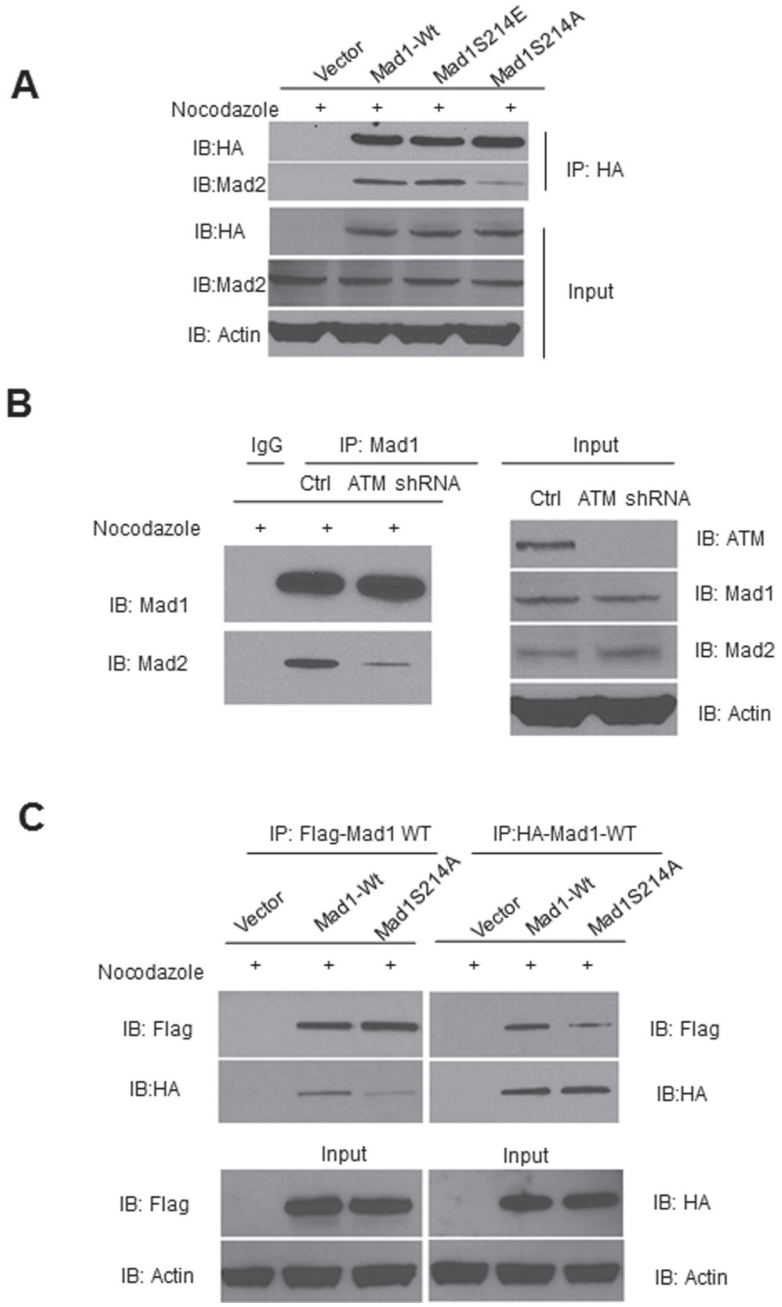

Fig. 3. Mad1 Serine 214 phosphorylation promotes Mad1 and Mad2 interactions. (**A**) HeLa cells were transfected with HA-tagged WT, S214A or S214E mutants of Mad1 and treated with nocodazole for 16 h. The exogenous proteins were immunoprecipitated with the anti-HA antibody followed by immunoblotting using indicated antibodies. (**B**) Endogenous Mad1 were immunoprecipitated from cells with stably infected cells with control shRNA or ATM shRNA. The immunoprecipitates were blotted with the indicated antibodies. (**C**) HeLa cells were cotransfected with HA-tagged and Flag-tagged WT or S214A of Mad1. Thirty-six hours later, cells were treated with nocodazole for 16 h. The exogenous proteins were immunoprecipitated with the anti-Flag or anti-HA antibody followed by immunoblotting using HA and Flag antibodies.

activation of the SAC. This observation echoes a recent report that Mad1 overexpression weakens mitotic checkpoint signaling by mislocalization of the Mad1 binding partner Mad2 (5). However, a serine to alanine substitution of Mad1 (S214A) appears to have a more inhibitory effect on activation of the SAC (Figure 2A). There are two possibilities behind this phenotype: (i) S214A has a dominant negative effect on endogenous Mad1. This is supported by our data in Figure 3A, in which S214A is capable of disrupting Mad1 homodimer formation, which might be crucial for the intact Mad1 function in mitosis. However, it is noted that S214A also showed less interactions with Mad2; therefore, the sequestration effect of Mad1 on Mad2 is expected to be diminished. (ii) It is also possible that S214A might be affecting the upstream ATM kinase activity, therefore causing a defect in the SAC. This is supported by the fact that S214A posed a less significant effect on the SAC in ATM knock-down cells (Figure 2D).

The functional significance of the ATM-Mad1 pathway has been demonstrated that overexpression of the S214A mutant Mad1 causes aneuploidy, indicating that the phosphorylation event contributes to the maintenance of chromosomal stability.

Molecular modeling has become a powerful tool that provides very useful structural information. Such structural insight at the atomic level is critical for the understanding of protein functions. Our structural model of a MAD1 fragment (Figure 5) indicates Serine 214 locates at the tip a relatively short loop region and is

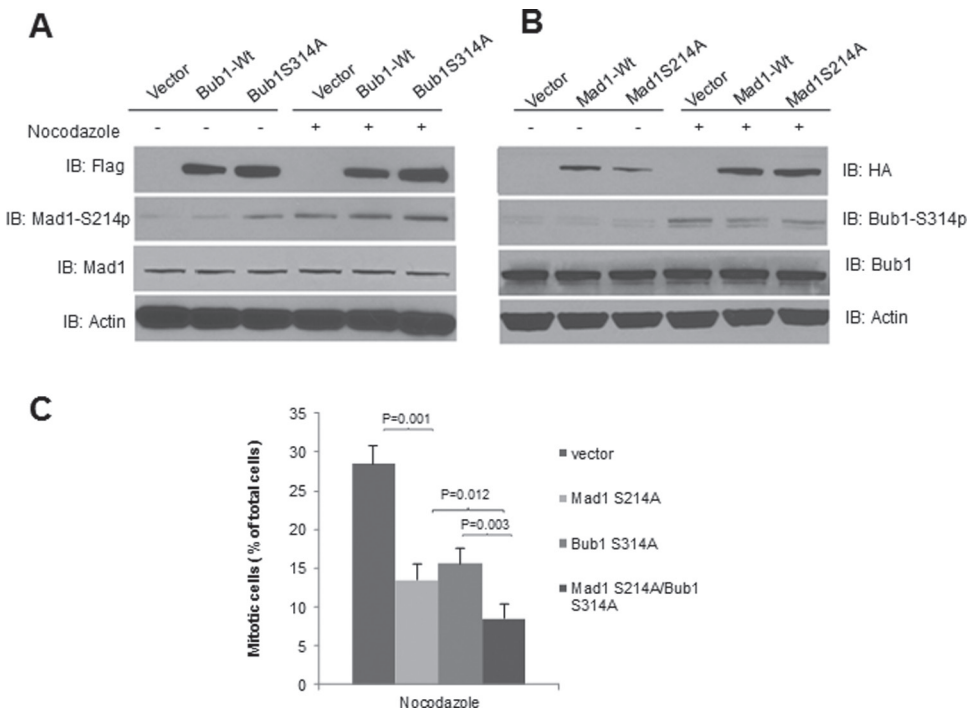

Fig. 4. ATM-mediated Mad1 and Bub1 phosphorylation functions independently to regulate the spindle checkpoint. (**A**) HeLa cells were transfected with vector, Flag-tagged WT or S314A mutants of Bub1 and treated with nocodazole for 16 h. Cells were then harvested and immunoblotted with indicated antibodies. (**B**) Cells were transfected with vector, HA-tagged WT or S214A mutants of Mad1 followed by treatment with nocodazole for 16 h. Cells were then harvested for immunoblotting with indicated antibodies. (**C**) Cells were transfected with vector, S214A Mad1 only, S314A Bub1 only or cotransfected with S214AMad1 and S314ABub1 plasmids. After nocodazole treatment (16 h), mitotic cells were analyzed by flow cytometry-based histone-H3-Ser10p staining. Mean mitotic percentages of at least triplicate samples are shown, and error bars represent the variations around the averages. Statistic analyses were done by *t*-test and *P* values are presented.

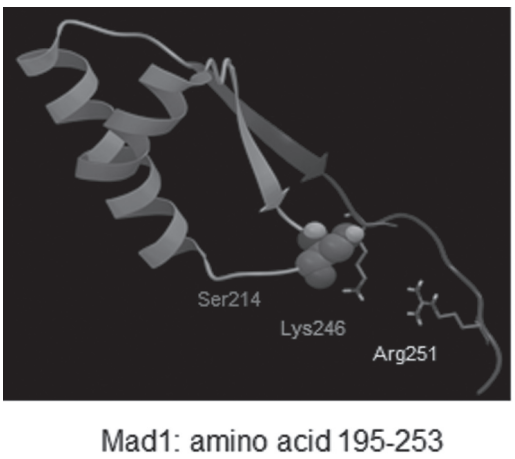

Fig. 5. The computational model of the Mad1 fragment (amino acid 195–253). Based on the crystal structure of pyruvate kinase (PDB ID: 1E0T), a homolog model was first generated using *PRIME*, the protein structure prediction module of Schrödinger®. This structural model of the Mad1 fragment was then further optimized using the protein preparation protocol for final analysis.

fully solvent-exposed, which enables Serine 214 to be accessible for phosphorylation. Although loop regions tend to be more flexible, the electrostatic interactions and a potential water-mediated hydrogen-bonding network formed between Serine 214 and the surrounding residues (K246/R251) stabilize the loop structure that keeps Serine 214 fully accessible. Although this structure model is consistent with our experimental conclusion that Serine 214 is important for Mad1 function, further experimental investigation, such as mutation of the surrounding residues as well as structural determination, will be needed to fully understand the mechanism.

The large-scale proteomic studies have identified several mitotic components as direct ATM targets in the DDR signaling (19). We have demonstrated that Bub1 Serine 314 and Mad1 Serine 214 can be phosphorylated by ATM in mitosis. We attempted to explore whether there was a sequential effect on ATM-mediated Bub1 and Mad1 phosphorylations. The results suggest that these phosphorylation events are independent of each other. However, coexpression of these phosphorylation depleting mutants showed a more drastic effect on the SAC, indicating that both ATM-mediated phosphorylation events contribute parallel to an optimal activation of the checkpoint.

Besides its well-characterized role as a major DDR kinase, the evidence of the mitotic function further supports ATM's role in the maintenance of genomic and chromosomal stability (22). Although mitotic ATM activation is not as dramatic as in the DNA double-strand break response, it is expected that mitotic cells undergoing DNA damage might be influenced by ATM function; therefore, inhibiting ATM in the presence of DNA damage might lead to an increase mitotic cell death.

Collectively, our data presented here demonstrate that mitotically activated ATM phosphorylates Mad1 on Serine 214 to facilitate the activation of the SAC by promoting Mad1 homodimerization and heterodimerization with Mad2.

Supplementary material

Supplementary Figures 1–3 can be found at http://carcin.oxfordjournals.org/.

Funding

National Institutes of Health (R01CA133093, R01ES016354, R21NS061748 to B.X.).

Acknowledgements

We thank Dr Sankar Mitra for helpful comments on the manuscript. We thank Kathryn Brinkman and Rebecca Boohaker for proof-reading of the manuscript. Time-lapse imaging was performed at the HMRI Advanced Cellular and Tissue Microscope Core Facility. Flow cytometry was conducted at the University of Alabama at Birmingham Comprehensive Cancer Center and the HMRI Flow Cytometry Core.

Conflict of Interest Statement: None declared.

References

1. Burke,D.J. (2000) Complexity in the spindle checkpoint. *Curr. Opin. Genet. Dev*., **10**, 26–31.
2. Bharadwaj,R. *et al*. (2004) The spindle checkpoint, aneuploidy, and cancer. *Oncogene*, **23**, 2016–2027.
3. Amon,A. (1999) The spindle checkpoint. *Curr. Opin. Genet. Dev*., **9**, 69–75.
4. Brady,D.M. *et al*. (2000) Complex formation between Mad1p, Bub1p and Bub3p is crucial for spindle checkpoint function. *Curr. Biol*., **10**, 675–678.
5. Ryan,S.D. *et al*. (2012) Up-regulation of the mitotic checkpoint component Mad1 causes chromosomal instability and resistance to microtubule poisons. *Proc. Natl. Acad. Sci. U. S. A*., **109**, E2205–E2214.
6. Iwanaga,Y. *et al*. (2007) Heterozygous deletion of mitotic arrest-deficient protein 1 (MAD1) increases the incidence of tumors in mice. *Cancer Res*., **67**, 160–166.
7. Jin,D.Y. *et al*. (1998) Human T cell leukemia virus type 1 oncoprotein Tax targets the human mitotic checkpoint protein MAD1. *Cell*, **93**, 81–91.
8. Chi,Y.H. *et al*. (2008) Requirements for protein phosphorylation and the kinase activity of polo-like kinase 1 (Plk1) for the kinetochore function of mitotic arrest deficiency protein 1 (Mad1). *J. Biol. Chem*., **283**, 35834–35844.
9. Kim,S. *et al*. (2012) Structure of human Mad1 C-terminal domain reveals its involvement in kinetochore targeting. *Proc. Natl. Acad. Sci. U. S. A*., **109**, 6549–6554.
10. Haller,K. *et al*. (2006) The N-terminus of rodent and human MAD1 confers species-specific stringency to spindle assembly checkpoint. *Oncogene*, **25**, 2137–2147.
11. Kastan,M.B. (2008) DNA damage responses: mechanisms and roles in human disease: 2007 G.H.A. Clowes Memorial Award Lecture. *Mol. Cancer Res*., **6**, 517–524.
12. Yang,C. *et al*. (2011) Aurora-B mediated ATM serine 1403 phosphorylation is required for mitotic ATM activation and the spindle checkpoint. *Mol. Cell*, **44**, 597–608.
13. Chabalier-Taste,C. *et al*. (2008) BRCA1 is regulated by Chk2 in response to spindle damage. *Biochim. Biophys. Acta*, **1783**, 2223–2233.
14. Xiong,B. *et al*. (2008) BRCA1 is required for meiotic spindle assembly and spindle assembly checkpoint activation in mouse oocytes. *Biol. Reprod*., **79**, 718–726.
15. Stolz,A. *et al*. (2010) The CHK2-BRCA1 tumour suppressor pathway ensures chromosomal stability in human somatic cells. *Nat. Cell Biol*., **12**, 492–499.
16. Futamura,M. *et al*. (2000) Potential role of BRCA2 in a mitotic checkpoint after phosphorylation by hBUBR1. *Cancer Res*., **60**, 1531–1535.
17. Zachos,G. *et al*. (2007) Chk1 is required for spindle checkpoint function. *Dev. Cell*, **12**, 247–260.
18. Yang,C. *et al*. (2012) The kinetochore protein Bub1 participates in the DNA damage response. *DNA Repair (Amst)*., **11**, 185–191.
19. Matsuoka,S. *et al*. (2007) ATM and ATR substrate analysis reveals extensive protein networks responsive to DNA damage. *Science*, **316**, 1160–1166.
20. Nasmyth,K. (2005) How do so few control so many? *Cell*, **120**, 739–746.
21. Maldonado,M. *et al*. (2011) Constitutive Mad1 targeting to kinetochores uncouples checkpoint signalling from chromosome biorientation. *Nat. Cell Biol*., **13**, 475–482.
22. Boohaker,R.J. *et al*. (2014) The versatile functions of ATM kinase. *Biomed. J*., **37**, 3–9.

Received September 13, 2013; revised March 31, 2014; accepted April 4, 2014